Cement and Concrete Research 81 (2016) 112–121

Contents lists available at ScienceDirect

Cement and Concrete Research

journal homepage: www.elsevier.com/locate/cemconres

Influence of superabsorbent polymers on the surrounding cement paste

Fazhou Wang [a,*], Jin Yang [a], Shuguang Hu [a], Xinping Li [b], Hua Cheng [c]

[a] State Key Laboratory of Silicate Materials for Architecture, Wuhan University of Technology, Wuhan 430070, China
[b] School of Civil Engineering and Architecture, Wuhan University of Technology, Wuhan 430070, China
[c] Department of Military Civil Engineering, Logistical Engineering University, Chongqing 400016, China

ARTICLE INFO

Article history:
Received 8 February 2015
Accepted 8 December 2015
Available online 5 January 2016

Keywords:
Superabsorbent polymers
Interfacial transition zone
Hydration
Pore structure
Microhardness

ABSTRACT

In the last decade, the influence of superabsorbent polymers (SAP) on the performance of cementitious materials has been studied extensively. However, the formation mechanism and properties of the affected zone around SAP are still not well understood. Spherical SAP particles of a large size (1.5–2 mm) were used in this study to magnify the zone influenced by SAP. Hydration characteristics, capillary pore structure, microhardness and microstructure of the affected zone were investigated. The degree of hydration of the affected zone is higher than the unaffected zone by about 5%, an equivalent of an increase in w/c by 0.04. Capillary porosity is increased at early age, but reduced at later age, due to the desorption process of SAP. Results on the microhardness, the degree of hydration and the pore structure of the affected zone indicate a dense transition zone is produced in the presence of SAP.

1. Introduction

In the past few decades, high-performance concrete (HPC) with a low w/c ratio (w/c<0.4) has witnessed huge development thanks to the wide use of chemical admixtures and supplementary cementitious materials (SCM), such as the polycarboxylate superplasticizer and silica fume. Powers' model [1,2] suggests that cement could only hydrate completely with a w/c ratio above 0.42 [1]. The w/c ratio is generally above 0.38 for a normal concrete, and is between 0.20 and 0.38 for HPC [3]. Concretes with a low w/c ratio are very susceptible to cracking caused by autogenous shrinkage associated with the self-desiccation [4]. SAP are introduced into HPC as an internal curing agent, and the stored moisture in the SAP serves as water reservoirs which will be released during concrete hardening [5].

Benefits from the application of SAP in concrete generally include humidity regulation, shrinkage mitigation, cracking reduction, etc. According to a series of studies, performances of concrete are influenced considerably by SAP. For workability, it was believed that the plastic viscosity of concrete was increased by the presence of dry SAP particles, which would accordingly influence the rheological behavior of fresh concrete [6]. For shrinkage, it was suggested that SAP could reduce the plastic shrinkage [7], autogenous shrinkage [8] and drying shrinkage [9]. For mechanical properties, SAP was often found to have a negative effect on the strength of concrete at early ages [10,11], whereas a higher strength at later ages was reported [12]. For durability, some studies showed that the introduction of SAP had almost no negative effect on the permeability [13,14], although a certain amount of pores were left in the hardened concrete by SAP. Furthermore, the freezing–thawing resistance of concrete was improved as a result of the increased void content [15]. However, to the knowledge of the authors, only a few studies [14,16–18] have been focused on the "affected zone" which is directly influenced by SAP in concrete. Characterization of the affected zone of SAP differs, depending on experimental techniques used [14]. Mechtcherine et al. [16] found that no differences were seen between the surrounding cement paste and the other matrix areas, by using backscattered electron (BSE) image. However, Lam [17] found a dark grayish rim which seemed like an interfacial transition zone (ITZ) around the SAP void, by using a BSE detector. Mönnig [18] also detected an affected zone with a thickness of 60 μm around the SAP particle, by observing the altitude profile changes compared to the reference layer.

The release of entrained water from SAP would have a significant effect on the properties of cement paste, such as the hydration process, the pore structure evolution, etc. According to some recent studies, the primary hydration heat peak occurred earlier compared to the corresponding pastes with the same water amount but without SAP [19], the cumulative heat of hydration and the ultimate degree of hydration were increased because of the release of water retained in SAP [19–22]. After the water release, extra voids were created, and the total porosity of the whole cement paste was increased [16,21]. It was also

* Corresponding author at: School of Materials Science and Engineering, Wuhan University of Technology, 122# Luoshi Road, Wuhan 430070, China. Tel.: +86 27 8764 2570; fax: +86 27 8765 1779.
E-mail address: fzhwang@whut.edu.cn (F. Wang).

http://dx.doi.org/10.1016/j.cemconres.2015.12.004
0008-8846/

reported that the water release continued the hydration of cement so that the porosity was decreased at late ages [23]. It should be noted that these existing studies were mostly focused on the whole cement paste with or without SAP, and were thus an overall representation. Investigations on the properties of the affected zone alone are still very few.

Reasons for the scarcity of research on the affected zone by SAP are mainly as follows: Firstly, the particle size of SAP usually used in concrete is a few hundred micrometers, thus the concomitant voids after water release of SAP are very small. This makes the potential ITZ around SAP very hard to distinguish. Secondly, some gel polymer SAP powders prepared after being dried by crushing produce irregular particles, thus producing irregular small voids in the concrete.

As a result, the present study used a large spherical SAP with a dry particle size of 1.5–2 mm which makes it more feasible to identity the affected zone [24]. Properties, such as hydration heat flow, degree of hydration, pore size distribution, microhardness and backscattered electron imaging of the affected zone around SAP and the unaffected zone were studied. It should be noted that the large size SAP which has been used is not practical for internal curing.

2. Materials and methods

2.1. Materials

Portland cement was used with a Blaine fineness of 360 m^2/kg and the following chemical composition in wt.% (SiO_2: 21.70, Al_2O_3: 4.76, Fe_2O_3: 3.57, CaO: 63.01, MgO: 2.12, and SO_3: 1.98). Its physical and mechanical properties were shown in Table 1. A polycarboxylate-based high-range water-reducing admixture with 23.5% solid content was used only for the disc-shaped specimen preparation.

Polyacrylicacid-based SAP spheres were used with a dry particle size of 1.5–2 mm, and 4–5 mm after swelling. The maximum water absorptivity of spherical SAP in pure water was 115 g/g SAP (Fig. 1). Large spherical SAP particles used in this study have a lower water absorptivity than the SAP powders (100–200 μm in dry particle size) commonly utilized for internal curing (Fig. 1), but they have similar desorption behavior in the cement paste affected by osmotic pressure and humidity gradient [24]. As a result, SAP particles were pre-soaked before use. All the presoaked SAP spheres used in this study had almost the same particle size which meant the same amount of absorbed water.

2.2. Specimen preparation

To create the spherical pores in the cement paste formed by SAP, a hemispherical SAP particle was positioned at the bottom of a culture dish, then fresh cement paste was slowly poured in to form the disc-shaped specimen with a thickness of 15 mm and a diameter of 85 mm. The cement paste mixtures with w/c ratios of 0.24, 0.26, 0.28, 0.30, 0.32 and 0.34 (all the w/c mentioned in this paper means nominal w/c), are mixed in a standard 2.5 L mixer for 2 min with a revolution speed of 62 ± 5 r/min, and another 2 min with a revolution speed of 126 ± 10 r/min, according to the Chinese national standard GB/T 1346-2011. The spherical SAP was pre-soaked in solutions with given concentration which would be discussed later. When red dye was added into the solution, it could also be used to track the water diffusion trace of SAP. The disc-shaped specimen was then sealed with plastic films

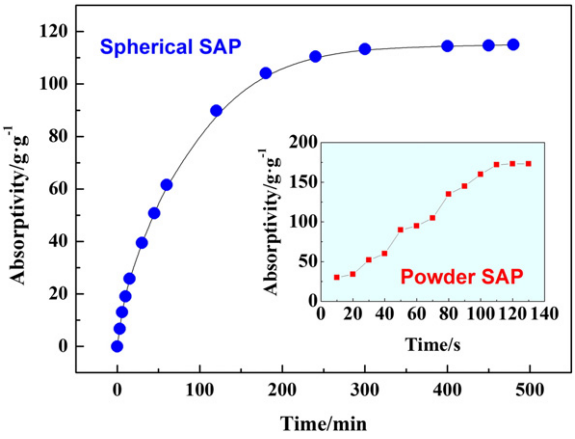

Fig. 1. Water absorption behavior of large SAP spheres and fine SAP powders in pure water.

to prevent moisture exchange, and cured at a temperature of 20 °C. The disc-shaped specimens were used to for the degree of hydration analysis, microhardness test, pore structure investigation and BSE imaging.

The disc-shaped specimen was shown in Fig. 2. The cement paste with SAP was divided into two zones: Section A and Section B. Section A means the affected zone close to SAP, and Section B indicates the unaffected zone which was not influenced by SAP. The following work mainly focused on the difference between the Section A and the Section B. The Section A and Section B could be distinguished by red dye, which was also described in [24].

2.3. Equilibrium concentration between SAP and cement paste

In this study, the spherical SAP particles were pre-soaked before mixing in the fresh cement paste. As we all know that the pre-absorptivity of SAP would affect the absorption/desorption behavior of SAP in cement paste dramatically. When the pre-absorptivity of SAP is lower than the equilibrium absorptivity (absorptivity of SAP in the pore solution), the SAP particles would absorb first and then release. When the pre-absorptivity is higher than equilibrium absorptivity, the SAP particles would always release. To simplify the original state of presoaked SAP spheres after mixing in the fresh cement paste, the SAP particles were presoaked with an equilibrium state so that the presoaked SAP would not absorb first or release too fast. In other words, the presoaked SAP would remain relatively steady until the concentration of pore solution goes up. Thus, the presoaked SAP spheres would only experience the desorption process, since this paper was focused on the effect of desorption on the zone around SAP.

The moisture exchange between SAP and solution is mainly controlled by osmotic pressure which is principally affected by the concentration of solution, as described by Eq. (1). In fact, the equilibrium state of presoaked SAP in the cement paste could be controlled by limiting the absorbing time if absorbed in distilled water, or using proper concentration if absorbed in solution, both to get the equilibrium absorptivity. In this study, sodium chloride solution with proper concentration was used to reach the equilibrium state in the cement paste. Solution with

Table 1
Physical and mechanical properties of cement.

Blaine specific surface (m^2/kg)	Surface density (g/cm^3)	Setting time (minute)		Compressive strength (MPa)	
		Initial set	Final set	3-day	28-day
360	3.01	130	210	35	62

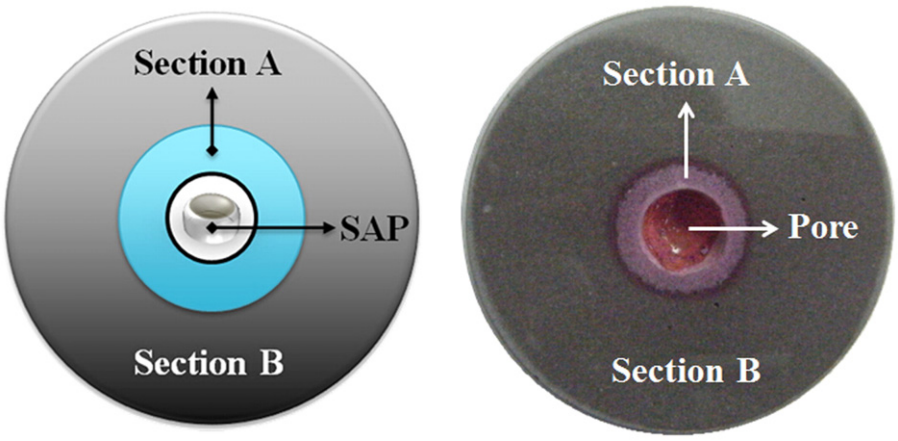

Fig. 2. Affected zone (Section A) and unaffected zone (Section B).

OH^-, $SO4^{2-}$, Ca^{2+} was not chosen because they would have some complicated effect on the hydration of cement as well as the polymer network. It should be noted that sodium chloride also has little effect on the hydration inevitably. However, it has the simple composition and all the SAP would be soaked in the sodium chloride solution with the same concentration, thus the accompanying effect would be ignored.

$$\prod = c_B RT \tag{1}$$

where Π is the osmotic pressure and c_B is the concentration of solution.

The test methods were as follows: First, the SAP particles were saturated in sodium chloride solutions with different concentrations (0, 0.4, 0.8, 1.2 mol/L); then, the saturated SAP particles were soaked in the cement paste filtrate after hydrating for 3 h. The cement paste filtrate was obtained by vacuum filtration. Selection of this time (3 h) was because the composition of the pore solution in cement paste remain stable for 6–7 h after this time [25–27], and the presoaked SAP would stay in an equilibrium state during this period. When there was no significant change in the mass of the saturated SAP particles in one salt solution, the concentration of which would be approximately regarded as the equilibrium concentration. In other words, the SAP presoaked with equilibrium concentration would reach an equilibrium state as soon as it was mixed in the cement paste.

2.4. Cement hydration characteristics

Cement hydration characteristics in the presence of SAP were studied by evaluating the heat of hydration from isothermal calorimetry and the non-evaporable water based on the loss-on-ignition (LOI).

(1) Heat of hydration.

A multi-channel isothermal calorimeter was used to study the influence of SAP on the early age hydration of cement. One key issue for this investigation lies in the design of the cement–SAP mixture such that the affected zone of SAP is approximately equal to the volume of surrounding cement paste. In this study, Eqs. (2–4) were used to calculate the amount of cement. The chemical shrinkage (CS_∞) was incorporated in Eq. (3) to compensate for the associated volume change.

As an example, when the radius of spherical SAP was 2.5 mm, an affected zone with a radius of 5.5 mm or with a diffusion distance of 3 mm was formed [24], and the chemical shrinkage of sufficiently hydrated cement was about 10%, as reported in [28]. The amount of cement was about 1.2 g in order that all the surrounding cement paste was within the affected zone of SAP which could be regarded as the affected zone. In addition, a neat cement paste was prepared without SAP which could be regarded as the unaffected zone as a control system. The detailed mix design for this section was shown in Table 2.

$$V_{Curing} = \frac{4}{3}\pi\left(R_{IC}^3 - R_{SAP}^3\right) \tag{2}$$

$$V_{Paste} = \left(\frac{m_C}{\rho_C} + \frac{m_C \bullet W/C}{\rho_W}\right)(1 - CS_\infty) \tag{3}$$

$$\left(\frac{m_C}{\rho_C} + \frac{m_C \bullet W/C}{\rho_W}\right)(1 - CS_\infty) = \frac{4}{3}\pi\left(R_{IC}^3 - R_{SAP}^3\right) \tag{4}$$

where V_{curing} is the volume of affected zone of spherical SAP; V_{paste} the volume of cement paste; R_{IC} the radius of affected zone; R_{SAP} the radius of SAP; m_c the needed cement mass; ρ_c the density of cement and ρ_w is the density of water.

(2) Degree of hydration.

The degree of hydration was determined for Sections A and B based on the measurement of non-evaporable water. Individual samples from four vertical positions of each section were tested. Extra care was needed to extract samples from the disk-shaped specimen (Φ85 mm × 15 mm). The samples from Section A were dig out artificially and carefully around the 4–5 mm spherical pores left by SAP.

Sample preconditioning involved oven drying at 105 °C for 24 h to remove the evaporable water. Then the sample was transferred to a resistance furnace at 1040 °C for 3 h. The amount of non-evaporable water was determined as the mass difference of the sample between 1040 °C and 105 °C. The cement loss on ignition was also taken into account in the calculation and the LOI of cement had been measured as 1.17%. Typically, the non-evaporable water content for well hydrated cement was

Table 2
Mix design for heat of hydration test.

Specimen	w/c	Water	Cement	Presoaked SAP
0.24-A	0.24	0.288	1.200	0.068
0.26-B	0.26	0.312	1.200	–
0.30-B	0.30	0.360	1.200	–

Note: 0.24-A means cement paste in the affected zone with a nominal w/c of 0.24, and so on.

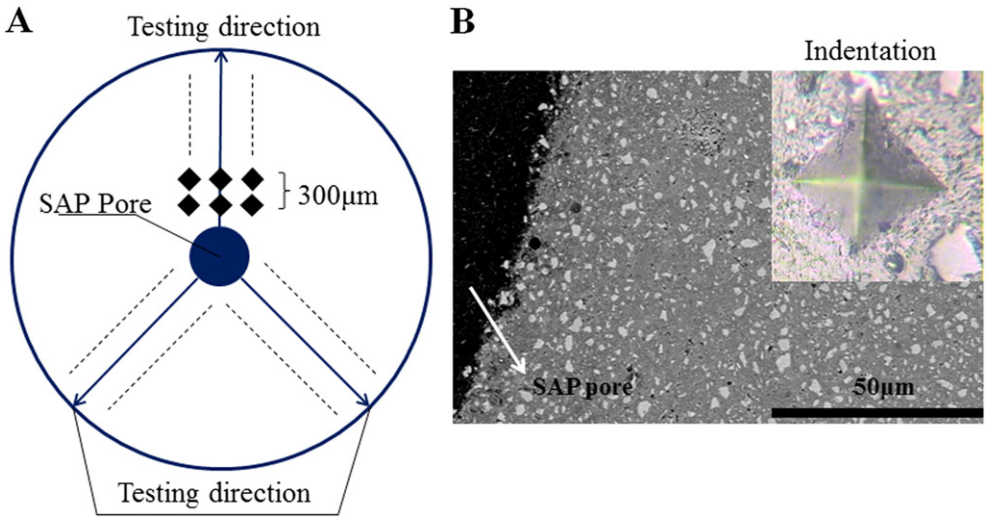

Fig. 3. Testing points (A) and indentation image (B) for microhardness test.

considered to be 0.23 g of water by 1 g of cement [29,30]. The degree of hydration can be estimated proportionally.

2.5. Pore structure analysis

The same sampling method was employed as the degree of hydration test. Prior to the test, the samples were fully degassed using a D-drying method [31]. A BELSORP-mini II made by Dutch Ankersmid company was used to measure the nitrogen adsorption and desorption isotherms at 77 K, with the relative pressure (P/P_0) of 10^{-4}–0.997. The specific surface area was determined using the BET method [32] within the P/P_0 range of 0.05–0.35. The pore size distribution was obtained from the adsorption and desorption isotherms using BJH method [33].

2.6. Microhardness test

The microhardness is a reliable method to evaluate the properties of interfacial transition zone [34,35]. In this study, the microhardness was measured on the affected and unaffected zones (see Fig. 2). A type HV-1000Z microhardness tester with a Vickers diamond pyramid indenter was used. The dried specimens (hydrated for 7 d and 28 d, w/c = 0.30) were impregnated with epoxy resin to protect the pore left by

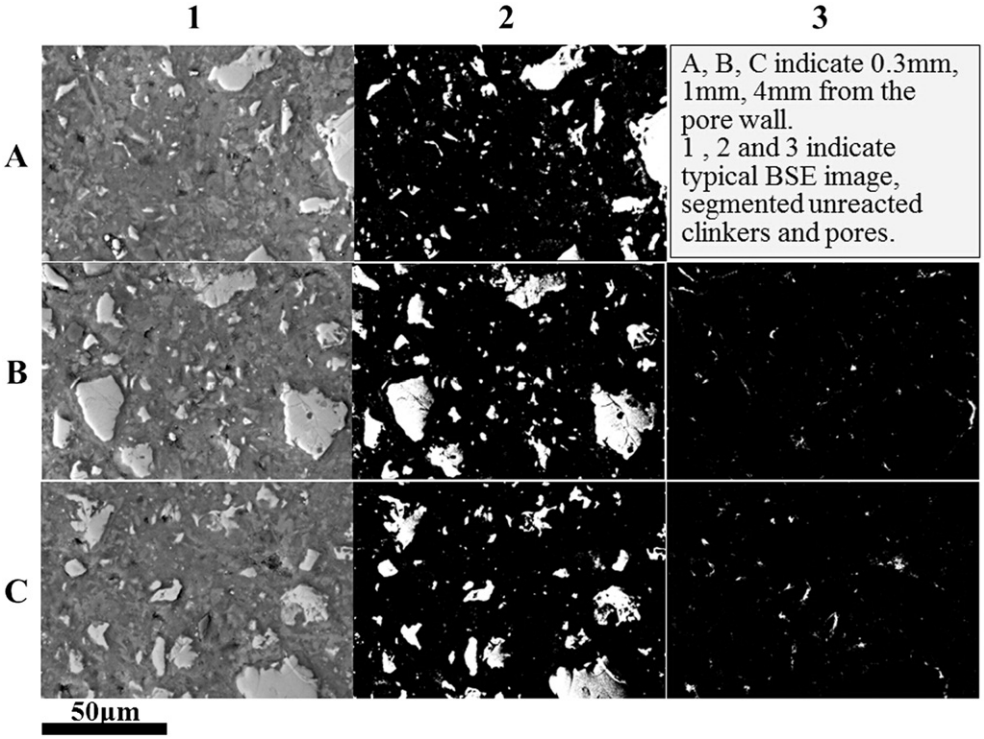

Fig. 4. BSE images and segmented images of cement pastes at different distances from the pore wall.

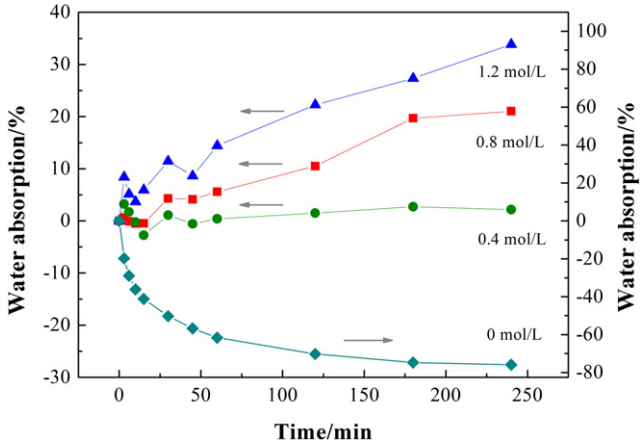

Fig. 5. Equilibrium concentration between SAP and cement paste.

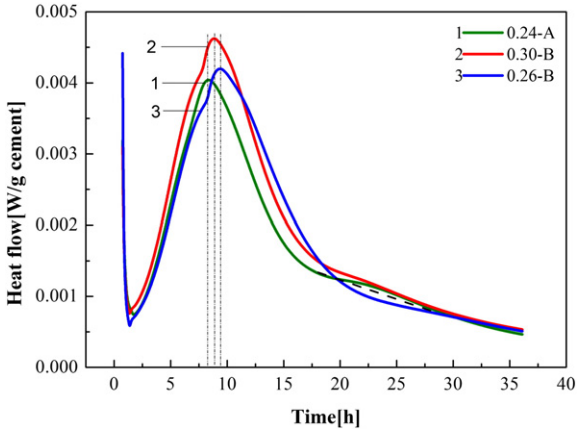

Fig. 7. Heat flow of cement paste with and without SAP.

SAP, and polished with 600, 800, 1200 and 2500 grit polishing papers and then polished using diamond abrasives of sizes 3, 1 and 0.25 μm, no water being used. Care was taken during the polishing not to damage the surface of the specimens. The microhardness of cement paste from the pore wall to the matrix was tested on the affected zone (Section A) and unaffected zone (Section B) to understand the micro mechanical difference between these two zones. The point near the pore edge was not tested to avoid the effect of potential polishing damage. Considering the large curing zone of the SAP particle, the measuring distance between the two neighboring testing points was chosen as 300 μm. The test was arranged in three different directions, and nine replicate indentations were tested for each distance, as shown in Fig. 3. The average values were used for calculating the Vickers hardness HV (MPa) by Eq. (5), in which P (kgf) is the applied force and D (mm) is the average of diagonals. A load of 0.2 kgf was applied with a dwell time of 10 s.

$$HV = \frac{2P\sin(136^{\circ}/2)}{D^2} \times 9.8 \quad (5)$$

2.7. Backscattered electron imaging

The specimen (hydrated for 28d, w/c = 0.30) preparation used for microhardness was also used for BSE imaging to understand the difference between the affected zone and unaffected zone. A FEI QUANTA FEG 450 ESEM fitted with a BSE detector was used. The microscope was operated at an accelerating voltage of 20 kV, with a working distance of 12 mm. Degree of hydration and porosity were analyzed by randomly collecting 50 images at each distance (0.3 mm, 1 mm, 4 mm) from the pore wall, with a magnification of 1000×. This magnification is used to obtain the fine pores with pore diameter below 100 nm. The images (Fig. 4) were digitized to 1536 × 1024 pixels, giving a field of view of 127 × 85 μm and a pixel spacing of 0.083 μm. The brightness and contrast of all the images were set for consistency.

The pore and unreacted cement area were segmented by binary image using grey-level thresholding, thus analyzing the porosity and the degree of hydration which had been clearly addressed by Wong et al. [36,37]. The porosity at the distance of 0.3 mm was not calculated because some damage of a narrow range close to the pore edge could not be avoided.

3. Results

3.1. Equilibrium concentration between SAP and cement paste

The saturated SAP particles pre-soaked in solutions with a series of different concentrations were immersed in the cement paste filtrate, and the weight change was monitored as shown in Fig. 5. It is evident that SAP pre-soaked in a salt solution with an ionic concentration of 0.4 M reaches the absorption/desorption equilibrium with the cement paste filtrate. As addressed in Section 2.3, this concentration could be regarded as the equilibrium concentration between SAP and cement paste. It should be noted that the following tests were started after this equilibrium had been reached.

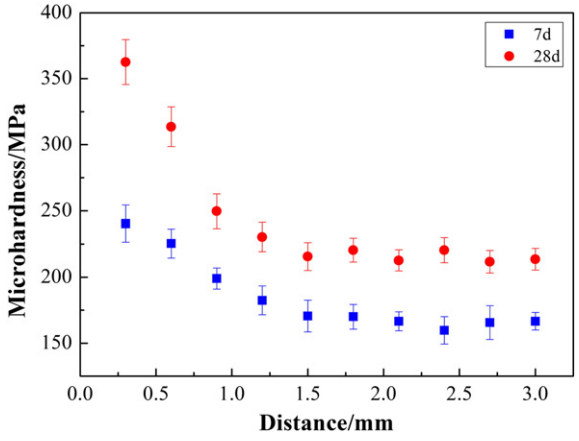

Fig. 6. Microhardness with different distance from the pore wall.

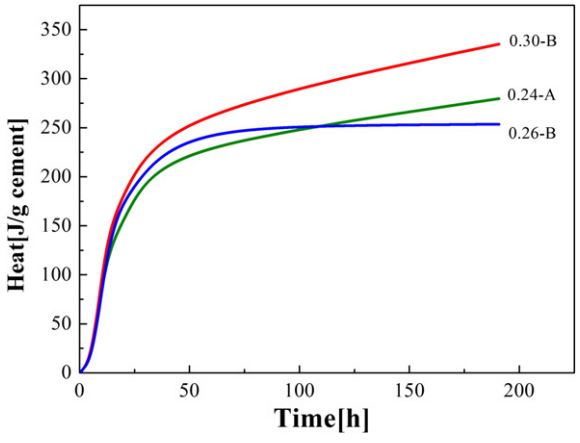

Fig. 8. Cumulative heat of cement paste with and without SAP.

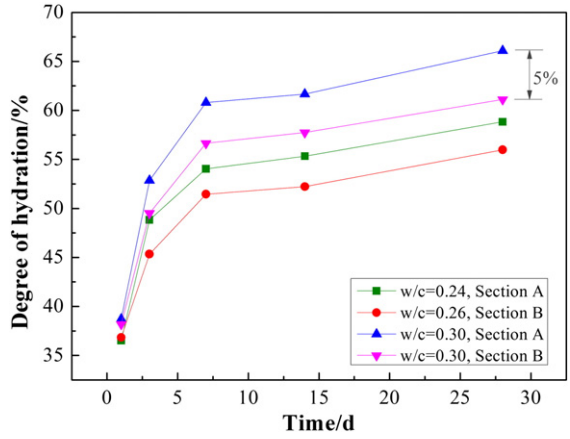

Fig. 9. Degree of hydration of cement paste with and without SAP for different w/c ratios.

3.2. Microhardness of the cement paste around SAP

The Vickers microhardness of the cement paste across Section A and Section B is shown in Fig. 6. The specimen cured for 28 days indicated a higher microhardness than that for 7 days. The microhardness decreased with the increased distance from the pore wall and flattened gradually. Generally speaking, Section A or the affected zone of SAP indicates a higher microhardness than Section B, no matter with 7 days hydration or 28 days hydration. This might be attributed to the difference in the degree of hydration and different microstructures (see the following Sections) between affected zone and unaffected zone.

3.3. Hydration of cement paste around SAP

The heat flow and cumulative heat are shown in Figs. 7 and 8, respectively, for affected zone and unaffected zone. It is observed that the primary peak of hydration heat is slightly advanced in the affected zone for the 0.24 w/c ratio paste, when compared with the reference paste with a w/c ratio of 0.26 (Fig. 7). In addition, its cumulative heat also exceeds that of the reference after around 100 h (Fig. 8).

The calculated degree of hydration for cement paste is increased at a higher w/c ratio, as seen in Fig. 9. The presence of the pre-soaked SAP particle clearly promotes cement hydration in Section A, exemplified by a 5% increase compared with Section B with the same w/c ratio. The enhancement of degree of hydration by SAP is in good agreement with the results reported in [20,22].

3.4. Pore size distribution of the cement paste around SAP

The pore size distribution (PSD) of Sections A and B is shown in Figs. 10 and 11 for two different w/c ratios (0.24 and 0.30). All the pore size distributions in the mesopore range present a similar multimodal characteristic, around 10 nm and 20 nm. The pore size parameters and distributions of cement paste around SAP pore are shown in Table 3.

Note: "0.24-3d-A" means paste of Section A, with a w/c ratio of 0.24, hydrated for 3 days, and so on.

4. Discussion

4.1. The formation of affected zone of SAP

The formation of affected zone or ITZ around SAP is directly associated with the desorption process of SAP. Thus, the desorption behavior of SAP in the cement paste will be addressed first. At the early age of hydration, the moisture exchange between SAP and cement paste is mainly induced by osmotic pressure [24]. It has been reported [25–27] that the total ionic concentration of cement paste increases rapidly to a certain value and then remains stable for several hours (6–7 h, for example). Thus, the presoaked SAP with an equilibrium concentration would stay in an equilibrium state during this period, in which almost no more moisture is exchanged between SAP and cement paste, as discussed in Sections 2.3 and 3.1. As cement hydration continues, there is a fast increase in the ionic concentration in pore solution, especially after the final set [26]. Thus, the equilibrium between SAP and cement paste is disturbed, and the desorption process of SAP particles commences in an environment of ions and humidity [24]. As shown in Fig. 12, the free water stored in SAP is released to the surrounding paste under the osmotic pressure (Π) caused by the increased concentration of pore solution, leading to the gradual formation of an annular curing zone, as shown in Fig. 2. Partial desorption of SAP would cause a volume contraction and create the spherical pore. This early-age desorption of SAP controlled by osmotic pressure will be discontinued upon the detachment between SAP and the pore wall. Thus, the remaining moisture in the SAP will be released to the paste under the humidity gradient (ΔRH) in the form of vapor (Fig. 12) for continuous curing in a later stage.

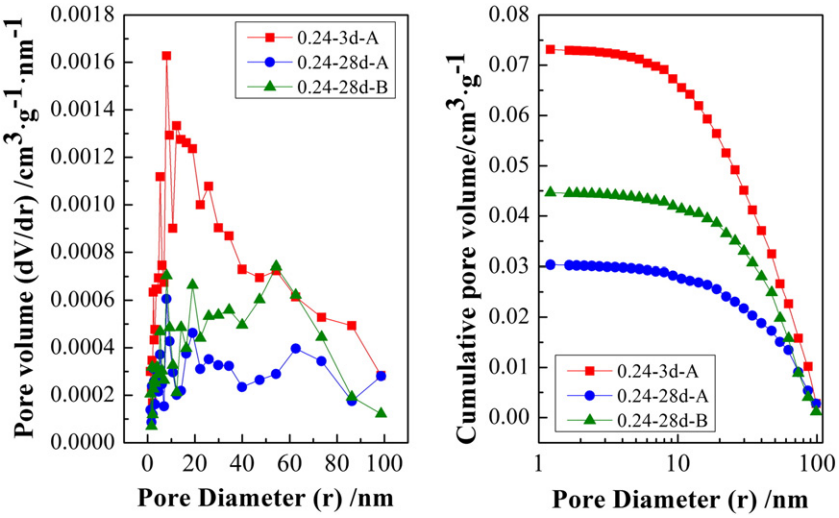

Fig. 10. PSD of affected zone and unaffected zone (w/c = 0.24).

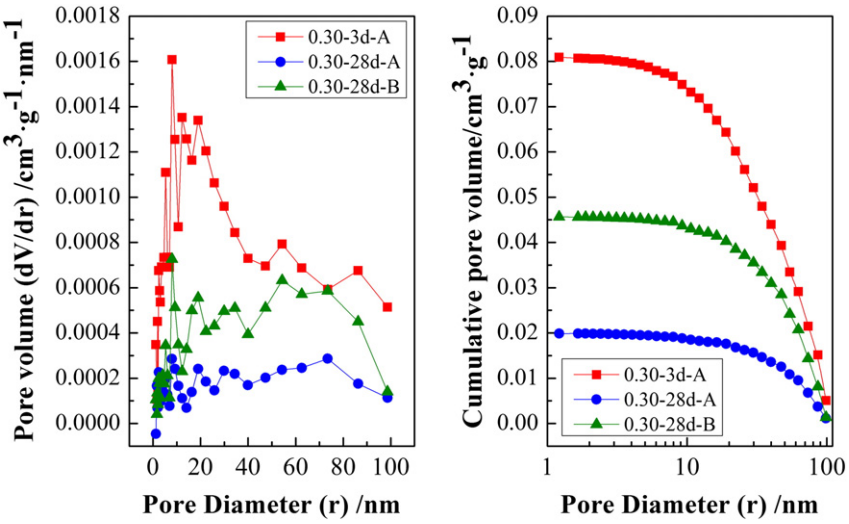

Fig. 11. PSD of affected zone and unaffected zone (w/c = 0.30).

4.2. Effect of SAP desorption on the ITZ

(1) Hydration of paste in ITZ.

The desorption of SAP would have an effect not only on the hydration heat flow (hydration heat release rate and cumulative heat) during the early age, but also on the degree of hydration of the whole cement paste during the late age [19]. In this study, the hydration heat release rate, cumulative heat and degree of hydration are discussed focusing on the affected zone and unaffected zone.

As discussed in Section 4.1, free water is released from the presoaked SAP to the fresh cement paste in the environment of ions during the early age of hydration. Besides the advanced primary peak of hydration heat, a pronounced shoulder is observed after hydrated for about 20 h on curve I (see Fig. 7), possibly indicating the release of entrained water from the SAP to the cement paste, and a similar phenomenon is also reported in [19] which is focused on the whole cement paste affected by SAP. This transient promotion in cement hydration is believed to be associated with the increased ionic concentration [25], as discussed in Section 4.1, which in turn accelerates the release of free water into the pore solutions [18,24]. This also helps explain the ultimate cumulative heat in affected zone exceeds that of unaffected zone after 100 h, as seen in Fig. 8.

The degree of hydration based on LOI of Section A is distinctly higher than Section B, and comparable to the effect of a higher w/c ratio (see Fig. 9). It is evident that the degree of hydration of Section A always exceeds the Section B almost by 5%, and is comparable with a higher w/c ratio, which is consistent with the results of hydration heat tests. Some existing studies [18,19] have reported that the effect of SAP entrainment on degree of hydration is similar to an increasing w/c ratio. However the magnitude of increase is still missing. It is found out in this study that the degree of hydration of Section A with a w/c ratio of 0.24 is between that of Section B with a w/c ratio of 0.26 and 0.30 (Figs. 8 and 9). To further confirm the effect of SAP on the surrounding cement paste, Section A with different w/c ratios is compared with Section B with the same or a higher w/c ratio, as shown in Fig. 13. It is interesting to find out that the degree of hydration of in Section A with a w/c of 0.24, 0.26, 0.28 and 0.30 is almost the same as that of Section B with a higher w/c ratio of 0.28, 0.30, 0.32 and 0.34, respectively. In other words, SAP entrainment is equivalent to increasing the w/c ratio by 0.04 in terms of the effect on the degree of hydration. Thus, the relationship of degree of hydration between Section A and Section B could be described by Eq. (6):

$$\alpha_A = \alpha_B + \alpha_{0.04} \tag{6}$$

where α_A is the degree of hydration of Section A; α_B is the degree of hydration of Section B; and $\alpha_{0.04}$ is the improved degree of hydration with an additional w/c of 0.04 in comparison to α_B. The $\alpha_{0.04}$ could be regarded as the degree of hydration contributed by SAP.

The necessary water entrainment for internal curing has been well discussed [1,38]. The calculated water demand of the cement and some experimental results in this study are shown in Table 4. It is indicated that the additional w/c ratio as a result of SAP is close to or slightly below the theoretical calculation for internal curing, when the nominal w/c ratio of cement paste is below 0.26. However, the value of difference between additional w/c contributed by SAP and the calculated water entrainment is increased by almost 0.01 when the nominal w/c ratio is higher. Actually, the additional w/c produced by SAP increases slightly with the increasing nominal w/c, which may result from the

Table 3
Pore size parameters and distributions of cement paste around SAP.

Specimen no.	Total pore volume/$cm^3\ g^{-1}$	Average pore diameter/nm	Surface area/$m^2\ g^{-1}$	Pore volume fraction/%		
				<2 nm	2–50 nm	>50 nm
0.24-3d-A	0.0738	41.76	7.07	0.47	57.35	42.19
0.24-28d-A	0.0306	48.41	2.53	0.61	46.70	52.70
0.24-28d-B	0.0450	53.47	3.36	0.52	44.93	54.55
0.30-3d-A	0.0816	45.36	7.20	0.48	54.32	45.20
0.30-28d-A	0.0251	60.82	1.65	0.10	38.93	60.97
0.30-28d-B	0.0461	59.06	3.12	0.25	38.52	61.23

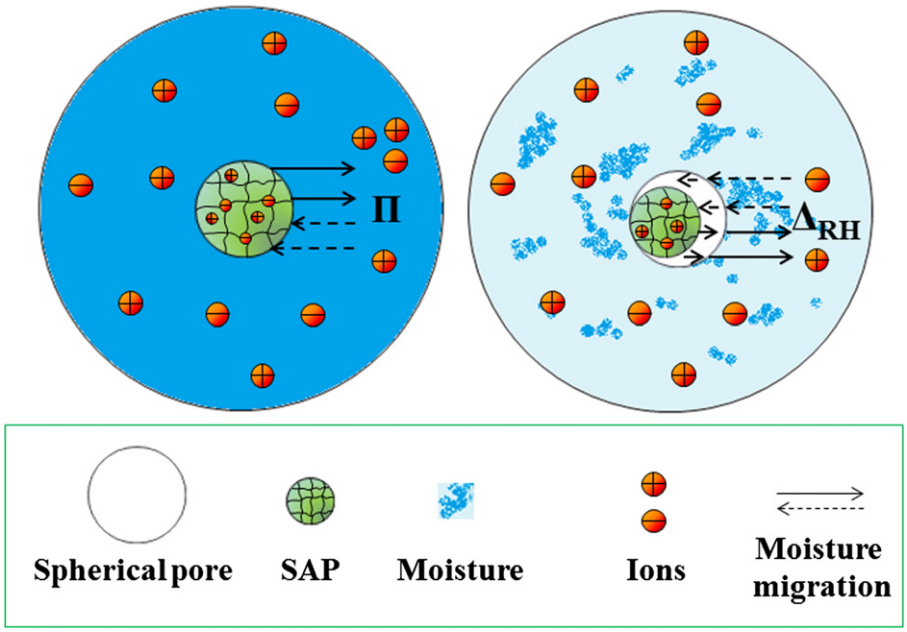

Fig. 12. Desorption process of SAP in the cement paste: osmotic pressure and humidity gradient.

effect of w/c on the desorption of SAP. Note that the magnitude of difference in degree of hydration between Section A and Section B is a rough estimate and not accurate enough in this study and further investigate should be carried out. It should also be noted that the desorption behavior of SAP in the cement paste could be potentially influenced by several factors, such as the w/c ratios, the entrained water content in SAP, the handling methods of SAP (dry mixed or presoaked), and so on, thus affecting the hydration of cement differently.

(2) Pore structure of ITZ.

MIP method had been widely used to investigate the pore structure of the whole cement paste modified by SAP [16,21]. In this Section, BET method is used to investigate the capillary pore structure of cement paste influenced by SAP, which has also been used by some other researchers [31,39], but not in internal curing field.

It should be noted that not all the water retained by SAP participates in the hydration of cement instantaneously. Actually, some of the released water diffuses into the cement paste and turns into capillary pores finally, let alone the voids left by SAP itself. Thus the desorption of SAP dramatically influences the capillary pore structure of the surrounding cement paste (see Figs. 10 and 11). The pore volumes (especially the mesopores) of Section A are relatively high when hydrated for 3 days, this is believed to be associated with the early desorption of SAP controlled by the osmotic pressure, which results in the diffusion of free water to the surrounding paste. In a sense, the formation of capillary pores are directly related to the excess water (free water) in cement paste [40]. As shown in Table 3, the released free water

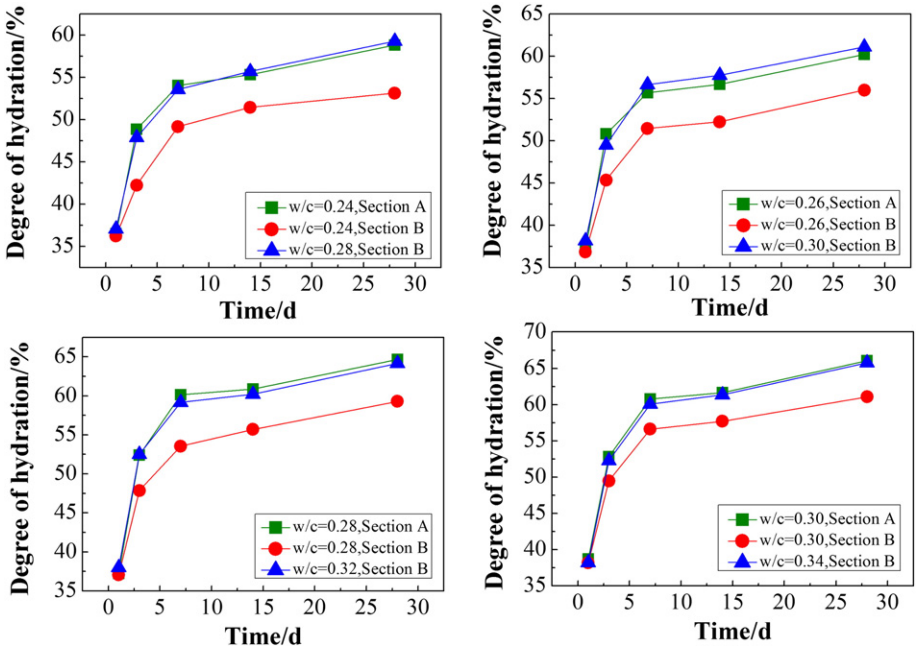

Fig. 13. Comparison of Section A and Section B with different w/c ratios.

Table 4
Computed $(w/c)_e$ and additional w/c produced by SAP.

Section A		Section B		Additional w/c produced by SAP	Calculated water demand
w/c	Degree of hydration,%	w/c	Degree of hydration,%		
0.24	58.8	0.28	59.3	Slightly below 0.04	0.043
0.26	60.2	0.30	61.1	Slightly below 0.04	0.047
0.28	64.7	0.32	64.2	Slightly above 0.04	0.050

obviously increases the volume of fine pores (<20 nm), and decreases the average pore diameter. As the hydration proceeds, fine pores could be filled by hydration products more easily, thus increasing the average pore diameter gradually, consistent with results in [23], using a back scatter electron (BSE) image analysis. As shown in Figs. 10 and 11, the total pore volume of Section A is decreased obviously after hydrating for 28 days, even lower than that of Section B, which is also demonstrated clearly in Table 3. This could be related to the continuous curing of vapor by SAP in a later stage, as discussed in Section 4.1. Part of the free water released by SAP at early stage would finally turn into capillary pores, thus going against the structural compactness of the cement paste. Herein, it would be more beneficial for the internal curing efficiency when the stored water in SAP is released to the hardened cement paste in a form of vapor which would not turn into capillary pores. Considering from this point, the desorption process of SAP could be somehow controlled in the cement paste, thus less moisture is released in the early stage controlled by osmotic pressure in a form of free water, and more moisture will be released in the late stage controlled by humidity gradient in a form of vapor, which would benefit the internal curing.

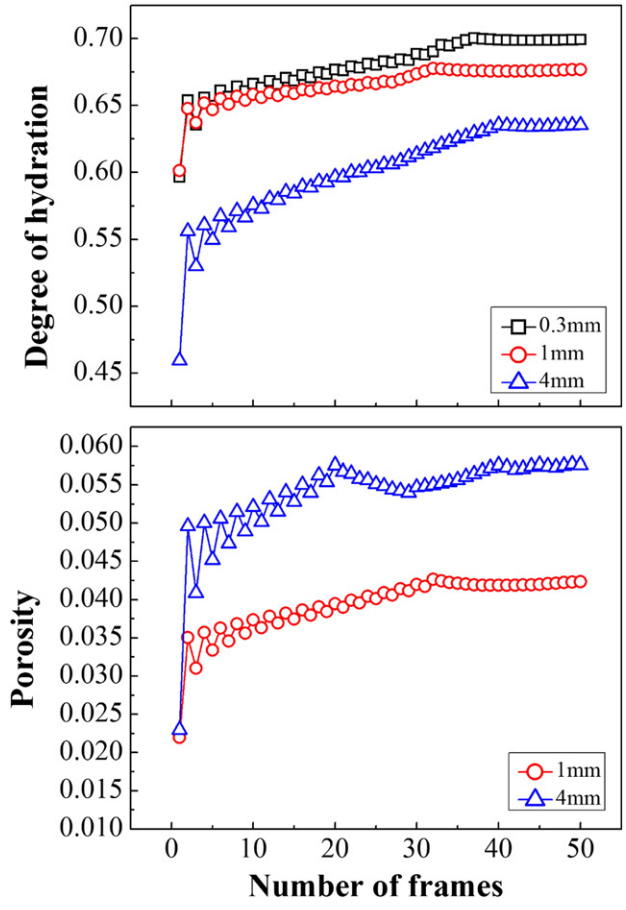

Fig. 14. Variation of average degree of hydration and porosity with the number of frames analyzed.

It could be concluded that the early desorption of SAP controlled by osmotic pressure markedly increases the pore volume and surface area of the surrounding cement paste. However, the pore volume and surface area are dramatically decreased in the late age, by the late desorption of SAP controlled by humidity gradient. Accordingly, the internal curing of SAP improves the hydration of cement paste around the voids left by SAP, and decreases the capillary porosity, thus forming a more dense annular curing zone. This is different from the ITZ around normal aggregates [41], but somewhat similar to the ITZ around lightweight aggregates [42].

(3) Backscattered electron image analysis.

The results of image analysis on BSE images are less reliable than results obtained by more traditional techniques [43], however it is convenient to study the paste at different distance from the pore wall and get a general variation trend of degree of hydration and porosity, which could be hardly realized by some traditional techniques, for example, LOI and BET. The variation trend might be difficult to recognize by unaided viewing from the BSE images (see Fig. 4), but it could be achieved by statistical approaches. The change in the average degree of hydration and porosity with the number of frames is shown in Fig. 14. It is observed that the degree of hydration decreases as the distance from the pore wall increases, indicating an enhancement of hydration of the affected zone. The degree of hydration by image analysis at distance of 0.3 mm (Section A), 1 mm (Section A) and 4 mm (Section B) is about 70.0%, 67.7% and 63.6% respectively, while the value by LOI at Section A and Section B is about 66.1% and 61.1% respectively. Generally, these two methods correspond well and indicate a similar trend.

The porosity in Fig. 14 ranges from 4.2% (Section A) to 5.8% (Section B), which is substantially lower than the values obtained by BET method. This is not surprising because the image resolution in this study is about 83 nm and pores smaller than the image resolution are excluded. However, the porosity from image analysis still indicates a similar trend with the result of BET that porosity in the affected zone is lower than the unaffected zone at 28 days.

Both of the trends of degree of hydration and porosity from Section A to Section B correspond well with the traditional tests discussed above. The enhanced hydration and decreased porosity are again proved to be consistent with the influence of desorption of SAP which would not be repeated again here.

(4) Micro-mechanical properties of ITZ.

According to the results on the degree of hydration and pore structure, the desorption of SAP obviously promotes the hydration of its surrounding cement paste (see Figs. 8, 13 and 14), and reduces the capillary porosity ultimately (see Figs. 10, 11 and 14), which would enhance the structural compactness and micro-mechanical performance (see Fig. 6) in the affected zone. Herein, although voids are left in the paste by SAP after desorption, the released vapor controlled by humidity gradient enhances the internal curing effect to promote the hydration of the surrounding paste and form a dense pore wall which would in turn compensate the negative effect of the voids on the strength [19].

5. Conclusions

The present study discusses the formation of affected zone around SAP, using large spherical SAP particles with a dry particle size of 1.5–2 mm to magnify the zone influenced by SAP. The hydration kinetics, degree of hydration, capillary pore structure, microhardness and microstructure of the affected zone are also discussed, based on the desorption behavior of SAP in cement paste.

The desorption of SAP promotes the hydration of its surrounding cement paste and advances the primary hydration heat peak. The degree of hydration based on LOI of cement paste around SAP is increased by about 5%, almost equal to an increase of w/c by 0.04. This is close to the theoretical calculation of necessary water entrainment for internal curing under specific w/c values.

The early desorption of SAP controlled by osmotic pressure markedly increases the capillary porosity of the affected zone. However, the late desorption of SAP controlled by humidity gradient reduces the ultimate porosity.

The trends of degree of hydration and porosity calculated from the BSE images are consistent with that tested by LOI and BET: the affected zone has a higher degree of hydration and lower porosity than the unaffected zone.

The microhardness of the affected zone is higher than the unaffected zone. This indicates a dense ITZ around SAP, which could be associated with the promoted hydration and decreased capillary porosity by the desorption of SAP.

Acknowledgements

The authors would like to express the appreciation to the financial supports from the National Natural Science Foundation of China (No. 51172173) and the Fundamental Research Funds for the Central Universities (No. 2014-IV-053).

References

[1] O.M. Jensen, P.F. Hansen, Water-entrained cement-based materials I: principles and theoretical background, Cem. Concr. Res. 31 (2001) 647–654.
[2] T.C. Powers, T.L. Brownyard, Studies of the Physical Properties of Hardened Portland Cement Paste, Bulletin 22, Research Laboratories of the Portland Cement Association, Chicago, 1948.
[3] B. Persson, Self-desiccation and its importance in concrete technology, Mater. Struct. 30 (5) (1997) 293–305.
[4] V. Mechtcherine, M. Gorges, C. Schroefl, A. Assmann, W. Brameshuber, A.B. Ribeiro, ... S. Zhutovsky, Effect of internal curing by using superabsorbent polymers (SAP) on autogenous shrinkage and other properties of a high-performance fine-grained concrete: results of a RILEM round-robin test, Mater. Struct. 47 (2014) 541–562.
[5] O.M. Jensen, P.F. Hansen, Water-entrained cement-based materials II: experimental observations, Cem. Concr. Res. 32 (2002) 973–978.
[6] O.M. Jensen, Use of Superabsorbent Polymers in Construction Materials, Proceedings of the First International Conference on Microstructure Related Durability of Cementitious Composites, Nanjing, China 2008, pp. 757–764.
[7] L. Dudziak, V. Mechtcherine, Enhancing early-age resistance to cracking in high-strength cement-based materials by means of internal curing using super absorbent polymers, additions improving properties of concrete, RILEM Proceedings PRO, 77 2010, pp. 129–139.
[8] F. Wang, Y. Zhou, B. Peng, Z. Liu, S. Hu, Autogenous shrinkage of concrete with super-absorbent polymer, ACI Mater. J. 106 (2009) 123–127.
[9] S. Mönnig, H.W. Reinhardt, Results of a comparative study of the shrinkage behavior of concrete and mortar mixtures with different internal water sources, in: O.M. Jensen, P. Lura, K. Kovler (Eds.), International RILEM Conference on Volume Changes of Hardening Concrete: Testing and Mitigation, RILEM Publications SARL 2006, pp. 67–75.
[10] B. Craeye, G. De Schutter, Experimental evaluation of mitigation of autogenous shrinkage by means of a vertical dilatometer for concrete, in: O.M. Jensen, P. Lura, K. Kovler (Eds.), International RILEM Conference on Volume Changes of Hardening Concrete: Testing and Mitigation, RILEM Publications SARL 2006, pp. 909–914.
[11] B. Craeye, M. Geirnaert, G.D. Schutter, Super absorbing polymers as an internal curing agent for mitigation of early-age cracking of high-performance concrete bridge decks, Constr. Build. Mater. 25 (1) (2011) 1–13.
[12] D.P. Bentz, M. Geiker, O.M. Jensen, On the mitigation of early age cracking, in: B. Persson, G. Fagerlund (Eds.), International Seminar on Self-Desiccation and Its Importance in Concrete Technology, Lund, Sweden 2002, pp. 195–204.
[13] H.W. Reinhardt, A. Assmann, Enhanced durability of concrete by superabsorbent polymers, Proc. BMC 9, Warsaw 2009, pp. 291–300.
[14] V. Mechtcherine, in: H.W. Reinhardt (Ed.), Application of Super Absorbent Polymers (SAP) in Concrete Construction, RILEM State of the Art Reports, 2, Springer 2012, pp. 115–134.
[15] A.E. Brüdern, V. Mechtcherine, Multifunctional use of SAP in strain-hardening cement-based composites, in: O.M. Jensen, M.T. Hasholt, S. Laustsen (Eds.), International RILEM Conference on Use of Superabsorbent Polymers and Other New Additives in Concrete, RILEM Publications SARL 2010, pp. 11–22.
[16] V. Mechtcherine, L. Dudziak, S. Hempel, in: T. Tanabe, et al., (Eds.), Mitigating Early Age Shrinkage of Ultra-High Performance Concrete by Using Super Absorbent Polymers (SAP), Creep, Shrinkage and Durability Mechanics of Concrete and Concrete Structures—CONCREEP-8, Taylor & Francis Group, London, UK 2009, pp. 847–853.
[17] H. Lam, Effects of internal curing methods on restrained shrinkage and permeability, PhD Thesis, University of Toronto, Toronto, 2005.
[18] S. Mönnig, Superabsorbing additions in concrete: applications, modeling and comparison of different internal water sources, PhD Thesis, University of Stuttgart, Stuttgart, 2009.
[19] J. Justs, M. Wyrzykowski, F. Winnefeld, D. Bajare, P. Lura, Influence of superabsorbent polymers on hydration of cement pastes with low water-to-binder ratio, J. Therm. Anal. Calorim. 115 (2014) 425–432.
[20] S. Zhutovsky, K. Kovler, Hydration kinetics of high-performance cementitious systems under different curing conditions, Mater. Struct. 46 (2013) 1599–1611.
[21] X. Kong, Z. Zhang, Z. Lu, Effect of pre-soaked superabsorbent polymer on shrinkage of high-strength concrete, Mater. Struct. 1-18 (2014).
[22] P. Lura, F. Durand, A. Loukili, K. Kovler, O.M. Jensen, Compressive strength of cement pastes and mortars with superabsorbent polymers, Int. RILEM Conference on Volume Changes of Hardening Concrete: Testing and Mitigation 2006, pp. 117–126.
[23] S. Igarashi, A. Watanabe, Experimental study on prevention of autogenous deformation by internal curing using super-absorbent polymer particles, Int. RILEM Conference on Volume Changes of Hardening Concrete: Testing and Mitigation, RILEM Proceedings PRO 52, RILEM Publications S. A. R. L. 2006, pp. 77–86.
[24] F. Wang, J. Yang, H. Cheng, J. Wu, X. Liang, Study on mechanism of desorption behavior of saturated superabsorbent polymers in concrete, ACI Mater. J. 112 (2015) 463–470.
[25] D. Rothstein, J.J. Thomas, B.J. Christensen, H.M. Jennings, Solubility behavior of Ca-, S-, Al-, and Si-bearing solid phases in Portland cement pore solutions as a function of hydration time, Cem. Concr. Res. 32 (2002) 1663–1671.
[26] B. Lothenbach, F. Winnefeld, Thermodynamic modelling of the hydration of Portland cement, Cem. Concr. Res. 36 (2006) 209–226.
[27] B. Lothenbach, F. Winnefeld, C. Alder, E. Wieland, P. Lunk, Effect of temperature on the pore solution, microstructure and hydration products of Portland cement pastes, Cem. Concr. Res. 37 (4) (2007) 483–491.
[28] M. Bouasker, P. Mounanga, P. Turcry, A. Loukili, A. Khelidj, Chemical shrinkage of cement pastes and mortars at very early age: effect of limestone filler and granular inclusions, Cem. Concr. Compos. 30 (1) (2008) 13–22.
[29] D.P. Bentz, K.K. Hansen, Preliminary observations of water movement in cement pastes during curing using X-ray absorption, Cem. Concr. Res. 30 (7) (2000) 1157–1168.
[30] G. Espinoza-Hijazin, M. Lopez, Extending internal curing to concrete mixtures with w/c higher than 0.42, Constr. Build. Mater. 25 (3) (2011) 1236–1242.
[31] A. Korpa, R. Trettin, The influence of different drying methods on cement paste microstructures as reflected by gas adsorption: comparison between freeze-drying (F-drying), D-drying, P-drying and oven-drying methods, Cem. Concr. Res. 36 (4) (2006) 634–649.
[32] S. Brunauer, P.H. Emmett, E. Teller, Adsorption of gases in multimolecular layers, J. Am. Chem. Soc. 60 (2) (1938) 309–319.
[33] E.P. Barrett, L.G. Joyner, P.P. Halenda, The determination of pore volume and area distributions in porous substances. I. Computations from nitrogen isotherms, J. Am. Chem. Soc. 73 (1) (1951) 373–380.
[34] S. Igarashi, A. Bentur, S. Mindess, Microhardness testing of cementitious materials, Adv. Cem. Basted Mater. 4 (2) (1996) 48–57.
[35] A.H. Asbridge, C.L. Page, M.M. Page, Effects of metakaolin, water/binder ratio and interfacial transition zones on the microhardness of cement mortars, Cem. Concr. Res. 32 (9) (2002) 1365–1369.
[36] H.S. Wong, N.R. Buenfeld, M.K. Head, Estimating transport properties of mortars using image analysis on backscattered electron images, Cem. Concr. Res. 36 (2006) 1556–1566.
[37] H.S. Wong, M.K. Head, N.R. Buenfeld, Pore segmentation of cement-based materials from backscattered electron images, Cem. Concr. Res. 36 (2006) 1083–1090.
[38] D.P. Bentz, K.A. Snyder, Protected paste volume in concrete: extension to internal curing using saturated lightweight aggregates, Cem. Concr. Res. 29 (1999) 1863–1867.
[39] M.C.G. Juenger, H.M. Jennings, The use of nitrogen adsorption to assess the microstructure of cement paste, Cem. Concr. Res. 31 (2001) 883–892.
[40] S. Mindess, J.F. Young, D. Darwin, in: R.K. Wu, X. Zhang, W. Yao, et al., (Eds.), Concrete, (Second Edition)Chemical Industry Press, Beijing, 2005 (Translation).
[41] J.P. Ollivier, J.C. Maso, B. Bourdette, Interfacial transition zone in concrete, Adv. Cem. Based Mater. 2 (1) (1995) 30–38.
[42] D.P. Bentz, Influence of internal curing using lightweight aggregates on interfacial transition zone percolation and chloride ingress in mortars, Cem. Concr. Compos. 31 (2009) 285–289.
[43] K.L. Scrivener, Backscattered electron imaging of cementitious microstructures: understanding and quantification, Cem. Concr. Compos. 26 (2004) 935–945.